Ground-Based Infrared Remote Sensing of Cloud Properties over the Antarctic Plateau. Part I: Cloud-Base Heights

Ashwin Mahesh,* Von P. Walden,+ and Stephen G. Warren

Geophysics Program and Department of Atmospheric Sciences, University of Washington, Seattle, Washington

ABSTRACT

A Fourier-transform interferometer, operated throughout 1992 at South Pole Station, measured downward spectral longwave radiance from 550 to 1500 cm^{-1} (7–18 μm) at a resolution of 1 cm^{-1}. Radiance measurements were usually made twice daily, coincident with routine launches of radiosondes made by the South Pole Weather Office; 223 radiance measurements (40% of the observations) were of cloudy-sky conditions. Cloud-base heights are retrieved from these data using a ground-based version of the radiance-ratioing method, which was originally developed to retrieve cloud-top heights from satellite data. Frequencies in the R branch of the 15-μm carbon dioxide band are used, exploiting the variation of atmospheric opacity with wavenumber. The annual cycle of cloud-base heights shows a bimodal distribution in all seasons except during the brief summer (December–January). Cloud-base heights are typically higher in the summer than in winter. Although retrieved cloud-base heights are uncorrelated with heights estimated by visual observers, both the retrieved and observed data indicate that base heights are bimodal. Most clouds have bases in the lowest few hundred meters, within the surface-based temperature inversion. The other mode is of higher clouds with base heights 1.5–3 km above the surface. Even the highest tropospheric clouds are within 6 km of the surface. Radiance ratioing can be used to detect polar stratospheric clouds, but their base heights are not reliably determined by the method.

1. Introduction

Retrievals of cloud properties from infrared satellite sensors are difficult over Antarctica because the snow surface is frequently at least as cold as the cloud, often making it difficult to identify a cloud, let alone infer its properties (Yamanouchi et al. 1987). Ground-based remote sensing methods have the advantage that the background is cold space, with brightness temperature much lower than that of the cloud. Ground-based remote sensing is therefore useful for determining the properties of clouds relevant to the energy budget and also for aiding the development of cloud-retrieval methods applied to satellite data. Mean climatic descriptions of cloud properties obtained from Antarctic data can be included in general circulation models (GCMs), providing a better representation of global climate. In the past, the validation of GCMs has been inhibited by the lack of long datasets from polar regions; the high latitudes are there-fore inadequately represented in these models (Simmonds 1990). More recent modeling work also suggests that proper inclusion of Antarctic cloud properties in these models is critical; significant changes in regional climate are observed when cloud properties are altered (Lubin et al. 1998).

Using Advanced Very High Resolution Radiometer channels at 11 and 12 μm, Lubin and Harper (1996) showed that outgoing longwave radiances over the Antarctic Plateau depend on effective cloud temperature, ice water path, and effective radius of the cloud particle size distribution. However, the relationships they obtained were limited by uncertainties and by lack of unique solutions to the radiative transfer equations. Retrieved solutions for cloud heights from satellite data are often multivalued in the polar regions because of surface-based temperature inversions (King et al. 1992). In this paper, we show that ground-based remote sensing can overcome this limitation, permitting clouds below the inversion to be distinguished from those above it. We present data through a complete seasonal cycle at South Pole Station. Because of the horizontal uniformity of the Antarctic Ice Sheet, the results are probably representative of a large area of East Antarctica.

2. Data

Moderate-resolution (1 cm^{-1}) infrared radiance spectra were measured using a Fourier-transform interfer-

---

* Current affiliation: Goddard Earth Sciences and Technology Center, NASA Goddard Space Flight Center, Greenbelt, Maryland.

+ Current affiliation: Department of Geography, University of Idaho, Moscow, Idaho.

Corresponding author address: Stephen G. Warren, Dept. of Atmospheric Sciences, Box 351640, University of Washington, Seattle, WA 98195-1640.
E-mail: sgw@atmos.washington.edu

ometer (FTIR) at viewing zenith angles of 45°, 60°, and 75° (Walden et al. 1998). The interferometer was located on the roof of a building on the upwind side of the station, 11 m above the snow surface, but the base heights reported here are given as height above the surface, not height above the instrument. The important sources of errors in the measurements were investigated by Walden (1995), namely, the radiance error induced by the uncertainties in the temperatures and emissivities of the calibration sources and by thermal instability of the interferometer. The estimated radiance error at wavenumber $\nu = 811$ cm^{-1} under clear skies is 1.5 RU, where RU is a "radiance unit," 1 mW m^{-2} sr^{-1} (cm^{-1})$^{-1}$. Above 5% of the radiance spectra were discarded as unreliable because of lack of thermal stability of the interferometer during an observation sequence, which lasted about 25 min.

If the radiance at 811 cm^{-1} exceeded 3 times the estimated radiance error at each viewing angle and also was larger than 5 RU (this threshold, at 75° and for typical particle sizes, corresponds to an optical depth of about 0.06), corresponding to a brightness temperature of 164 K, the scene was classified as "cloudy," otherwise it was "clear." Of the 516 measurements made during 1992, 223 observations met this threshold for cloud detection.

The radiance measurements were usually made twice daily, at about 1030 and 2230 UTC. These were the times of the routine radiosonde launches conducted by the South Pole Weather Office (SPWO) in summer (November–February). In winter, radiosondes were launched only once a day at 2230 UTC, so one-half of the wintertime FTIR observations were made close to the time of a radiosonde launch. The atmospheric temperature profile corresponding to each radiance measurement was determined by interpolation of the profiles from sondes launched before and after the radiance measurement. The temperature profiles were corrected for the thermal lag of thermistors on the radiosondes according to the method of Mahesh et al. (1997); this correction was necessary to remove errors in temperature as the sonde rises through steep inversions. For temperatures above 30 km, we used monthly average temperatures obtained by the *Upper Atmosphere Research Satellite* (*UARS*; Walden et al. 1997). Surface air concentrations of carbon dioxide (CO$_2$) at the South Pole were measured by the National Oceanic and Atmospheric Administration Climate Monitoring and Diagnostics Laboratory; monthly averages were used in this study. Although a ceilometer was operated by SPWO during 1992, we determined that data from that instrument were unusable, thus necessitating the determination of base heights from the spectral measurements themselves.

3. Radiative transfer calculations

For this paper, clear-sky radiances were calculated using the Line-By-Line Radiative Transfer Model
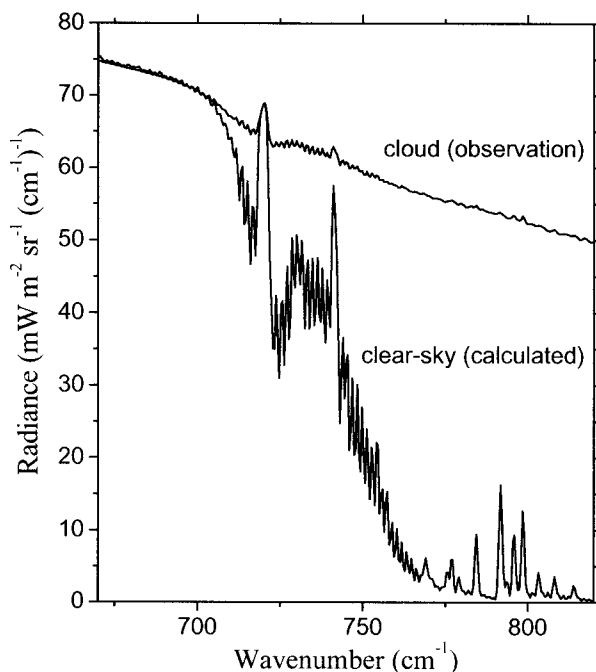

FIG. 1. Spectral radiance measurement under a cloud (on 26 Jan 1992) at the South Pole, with a simulated clear-sky spectrum calculated by a radiative transfer model. Near the center of the 15-μm band of carbon dioxide (667 cm^{-1}), the opacity of the atmosphere is very high, and most of the observed radiance is emitted from very close to the instrument. At these wavenumbers, radiance from the cloud is not detected by the instrument. With increasing distance from the center of the band, the opacity of the atmosphere decreases, and the spectrum of the cloudy sky is increasingly different from that of the clear sky.

(LBLRTM; Clough et al. 1992). Modifications were necessary to the LBLRTM subroutine "ALAYER," which calculates the path of refracted radiation through layers in a model atmosphere. In a very cold atmosphere with a steep near-surface temperature inversion, radiation was not properly refracted by ALAYER through the inversion layer. We therefore modified ALAYER for our particular application in consultation with the authors of the code (P. Brown and S. A. Clough 1998, personal communication).

Figure 1 shows a radiance measurement made under a cloud, along with a clear-sky spectrum computed using the ancillary data described above; only the *R* branch of the 15-μm CO$_2$ band is shown. At the center of the band (667 cm^{-1}), the two spectra are nearly identical. The opacity of the atmosphere in this region is very large so that most of the radiance received by the instrument is emitted within a few meters of it. At larger wavenumbers, the transmittance of the atmosphere increases, permitting photons from increasingly greater distances to reach the instrument. Until the *e*-folding absorption distance corresponding to the distance to the cloud base is reached, the two spectra remain similar. At even larger wavenumbers, the spectrum of the cloud is noticeably different from that of the clear sky. This

difference increases in the atmospheric window regions; at 811 cm^{-1}, the reference wavenumber used in our method, the clear-sky radiance is only a small fraction of the radiance from the cloud.

4. Retrieval of cloud-base pressure

a. Method

Variation of atmospheric transmittance with wavenumber in the 15-μm band of carbon dioxide has been used in the past to determine cloud-top heights. The "CO_2-slicing" method was introduced by Smith et al. (1974) to determine cloud-top heights from infrared spectral data taken from satellites (Chahine 1974; McCleese and Wilson 1976; Smith and Platt 1978; Menzel et al. 1983). The method was applied more recently to obtain cloud-top heights from high-resolution infrared spectral radiance data taken from aircraft (Frey 1988; Smith and Frey 1990). Wielicki and Coakley (1981) used the term "radiance ratioing" to describe this method, which describes the physical principle used in the CO_2-slicing method. We have modified this procedure for ground-based remote sensing of cloud-base heights.

The radiance-ratioing method relies on the fact that, within the 15-μm band of carbon dioxide, the average distance a photon travels is different at different wavenumbers. We define the e-folding distance at a particular wavenumber as the *vertical* distance into the atmosphere from which transmission to the surface is $1/e$. The e-folding distance therefore varies with viewing angle; examples are shown in Fig. 2a. The CO_2 band is used because CO_2 is a well-mixed gas, so that the e-folding distances do not change from one day to the next.

The wavenumbers that are best suited for detecting cloud-base heights are those that have e-folding distances comparable to the distance from the interferometer to the base of a typical cloud. At wavenumbers between 667 and 700 cm^{-1} the atmosphere is highly opaque, so that radiation reaching the surface comes from the nearby atmosphere rather than from the cloud base; correspondingly, the weighting functions for these wavenumbers are concentrated near the surface ($\nu =$ 681 cm^{-1} in Fig. 2b). Wavenumbers greater than about 755 cm^{-1} are less useful in determining the base heights of tropospheric clouds, because at these wavenumbers the e-folding distances of transmission into the atmosphere are greater than 100 km. The useful wavenumber range is therefore 700–755 cm^{-1}. In this range, e-folding distances correspond to heights in the troposphere at which clouds are often found. The e-folding distance is a function of the viewing zenith angle θ; therefore, different subsets of wavenumbers are useful in obtaining cloud-base heights from observations at different angles: 700–740 cm^{-1} at $\theta = 45°$, 700–748 cm^{-1} at $\theta = 60°$, and 700–755 cm^{-1} at $\theta = 75°$. These weighting functions have a different appearance than those typi-
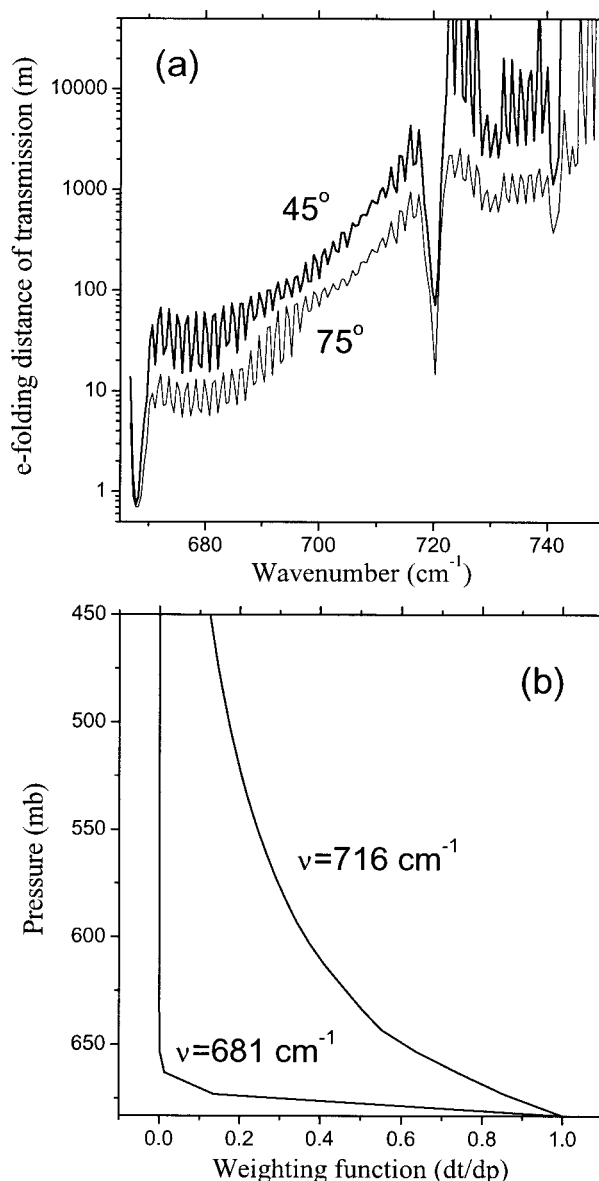

FIG. 2. (a) Variation in e-folding distance of transmission in the shortwave wing of the 15-μm CO_2 band, at viewing zenith angles of 45° and 75° for a summertime Antarctic atmosphere. The average distance that a photon travels before being absorbed increases from a few tens of meters at about 670 cm^{-1} to about 10 km at about 740 cm^{-1}. Radiance observed at the surface at these wavenumbers is therefore sensitive to clouds in the troposphere. (b) Normalized weighting functions for 681 and 716 cm^{-1}, shown for the atmosphere in Jan at a viewing zenith angle of 45°.

cally plotted for satellite views that shows a peak at some height within the atmosphere, but the difference in shape is simply due to a choice of vertical axis. When plotted versus pressure on a linear scale, the satellite-weighting functions peak at the top of the atmosphere, as our weighting functions peak at the surface.

Smith et al. (1974) showed that the observed radiance I_{obs} measured above or below a nonblack cloud can be

related to the radiance I_{clear} from the clear sky and to the radiance I_{bc} that would be emitted by a black cloud (emissivity equal to 1) at the same height. By taking the ratio of the difference of the observed and clear-sky radiances at two different wavenumbers ν and ν_0, the following relationship is obtained [derivations are given by Smith et al. (1974) and more recently by Frey (1988)]:

$$\frac{I(\nu, \theta)_{obs} - I(\nu, \theta)_{clear}}{I(\nu_0, \theta)_{obs} - I(\nu_0, \theta)_{clear}}$$

$$= \left[\frac{A\varepsilon(\nu, \theta)}{A\varepsilon(\nu_0, \theta)}\right]\left[\frac{I(\nu, \theta)_{bc} - I(\nu, \theta)_{clear}}{I(\nu_0, \theta)_{bc} - I(\nu_0, \theta)_{clear}}\right], \quad (1)$$

where ν is a wavenumber in the wing of the CO_2 band that is sensitive to cloud-base height, ν_0 is a reference wavenumber in the nearby window region where CO_2 absorption is much weaker, θ is the viewing zenith angle, A is the cloud cover fraction within the field of view of the instrument, and $\varepsilon(\nu)$ is the spectral emissivity of the cloud.

The reference wavenumber ν_0 is chosen to be as close to ν as is practical, so that $\varepsilon(\nu) \approx \varepsilon(\nu_0)$, which allows them to cancel in (1). (The method is thus designed to obtain the height even for thin clouds of low emissivity.) The variation of cloud emissivity between ν and ν_0 is a limitation of methods that use satellite data taken at specific channel wavelengths (e.g., Lubin 1994). Datasets with continuous spectra, such as those used here, allow the reference wavenumber to be chosen much closer to the wings of the CO_2 band, reducing errors caused by differences between $\varepsilon(\nu)$ and $\varepsilon(\nu_0)$.

Canceling the cloud fraction and spectral emissivities in (1), we obtain

$$\frac{I(\nu, \theta)_{obs} - I(\nu, \theta)_{clear}}{I(\nu_0, \theta)_{obs} - I(\nu_0, \theta)_{clear}} = \frac{I(\nu, \theta)_{bc} - I(\nu, \theta)_{clear}}{I(\nu_0, \theta)_{bc} - I(\nu_0, \theta)_{clear}}. \quad (2)$$

To calculate the cloud-base height, we calculate the two terms in (2) separately. The left-hand term,

$$\gamma \equiv \frac{I(\nu, \theta)_{obs} - I(\nu, \theta)_{clear}}{I(\nu_0, \theta)_{obs} - I(\nu_0, \theta)_{clear}}, \quad (3)$$

can be computed without specifying the cloud-base height; it requires only an observation and a clear-sky calculation. The right-hand term

$$R(p_c) \equiv \frac{I(\nu, \theta)_{bc} - I(\nu, \theta)_{clear}}{I(\nu_0, \theta)_{bc} - I(\nu_0, \theta)_{clear}}, \quad (4)$$

is a function of the cloud-base pressure p_c, where the radiance from a black cloud is computed as

$$I(\nu, \theta)_{bc} = B(T_c)t(p_c, p_s)$$
$$+ \int_{p_c}^{p_s} B[T(p)] \frac{d}{dp}t(p, p_s)\, dp, \quad (5)$$

where $B(T)$ is the Planck function for temperature T, T_c

is the cloud-base temperature, t is transmittance between two pressure levels, p_s is surface pressure, and p_c is the cloud-base pressure to be inferred. The first term, γ, is found by subtracting a clear-sky calculation from a spectral radiance measurement at two frequencies. The clear-sky calculation depends primarily on the atmospheric temperature structure, obtained from radiosonde data taken routinely at South Pole Station. Monthly average water vapor profiles are used in the calculation; however, because of the small amount of water vapor it contributes less than 5% of the total emission at frequencies between 700 and 755 cm^{-1}, so uncertainty in water vapor amount has little effect on our retrieved cloud-base height. The viewing zenith angle used in the calculation is the same as the one at which the radiance measurement was made.

The second term, $R(p_c)$, is a calculation assuming a black cloud at pressure p_c; p_c is varied until $R(p_c) = \gamma$, giving solution p_c for the cloud-base pressure. The transmittance in (5) is determined as follows. Using monthly average temperature and water-vapor profiles, the transmittances from the surface to many vertical heights in the atmosphere are computed for each wavenumber, yielding a matrix of transmittances. The instrument did not always stop at exactly the specified angle for each observation. However, the angle was recorded for each observation; for any given month it varied over roughly a 3° range. Therefore, we computed the transmission matrices at the extremes of the viewing angle as well as for the average viewing angle. Matrices for individual observations at a particular viewing angle were obtained by linear interpolation.

The quantity $R(p_c)$ is calculated for black clouds at many pressure levels within the troposphere; the cloud base is identified as the pressure at which γ is equal to R. An estimate of the cloud-base pressure is obtained at each wavenumber between 700 and 755 cm^{-1} at which the e-folding distance of transmission lies within the troposphere. The final estimate of cloud-base pressure is found in a second pass by weighting the initial estimates obtained at each wavenumber according to the estimated accuracy of each estimate, as follows. The slope of R versus p in a 10-hPa interval centered on the initial estimate of cloud-base pressure is determined at each wavenumber, and each estimate of cloud-base pressure is weighted by this slope. This is because a small slope means that a given uncertainty in R translates to a larger uncertainty in p. The highest weights are typically awarded to those wavenumbers whose e-folding distance of transmission into the atmosphere is close to the distance from the surface to the cloud base.

In many cases, the same cloud was observed at two or three viewing angles. The cloud-base pressure p_c is obtained at each angle, and, if the values of p_c are similar, the two or three values are averaged. Dissimilar values are interpreted as observations of different clouds at the different viewing angles. The radiosonde tem-
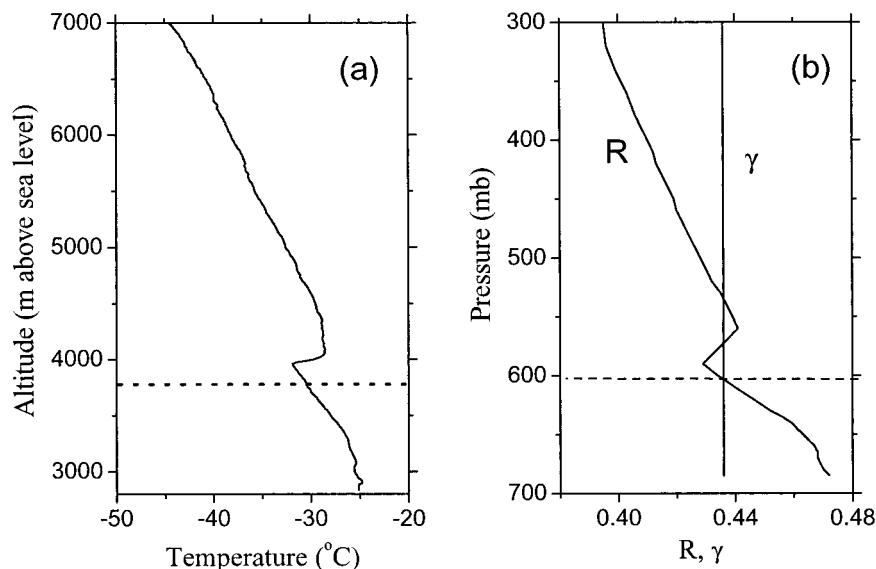
FIG. 3. Determination of cloud-base height in summer (26 Jan). (a) The radiosonde temperature profile suggests a cloud-top inversion 1200 m above the surface. The cloud-base height estimated visually by the SPWO is indicated by the dashed line. (b) Quantities R and γ, plotted vs pressure, are shown at a representative wavenumber (716 cm^{-1}). The solution nearest to the surface (marked by the horizontal dashed line) is the cloud-base height; the other two solutions correspond to points in the atmosphere at the same temperature, a condition that is caused by the inversion at 4000 m.

perature profile is then used to convert pressure p_c to base height z_b.

Figure 3a shows a summertime temperature profile in the lowest 3 km, plotted next to a graph of γ and $R(p_c)$ at a representative wavenumber of 716 cm^{-1}. The temperature profile shows a cloud-top inversion at 4000 m above sea level (1200 m above the surface). There are three values of p_c for which R is equal to γ. For this case, the first crossing of γ and R is chosen as the cloud-base pressure, designated by the horizontal dashed line. The following section describes how this solution was chosen.

b. Multiple solutions

In atmospheres with temperature inversions, multiple solutions of cloud-base height are often obtained, only one of which is correct. The difference in emissivity between the cloud and the overlying atmosphere often causes a cloud-top temperature inversion, which is seen in the temperature profile in Fig. 3a. In cases such as this one, the base of the cloud can be determined from the temperature profile as the solution at the highest pressure, closest to the surface. But a cloud at either of the other two pressures where $R = \gamma$ would result in the same measured radiance at this frequency. This situation of a cloud-top inversion is rare for Antarctic continental clouds; only a few thick summertime clouds in 1992 produced noticeable changes in the lapse rate. In winter, no cloud-top inversions were noticeable in the soundings.

A much more common situation is *surface-based* temperature inversions, which also cause multiple solutions (Fig. 4), but in this situation the choice of the correct cloud-base pressure is more difficult than for elevated inversions. On the Antarctic Plateau, strong surface-based temperature inversions occur throughout most of the year. This condition leads to two intersections of R with γ even if the data are perfect (and sometimes no intersection in real data with measurement errors). In such cases, the temperature profile is not helpful in determining the correct solution.

Figure 4 shows temperature profiles for 8 June and 7 July and plots of R and γ on these two days for two wavenumbers. Visual estimates by the SPWO place the cloud well above the top of the inversion on 8 June and within the inversion on 7 July. The temperature inversion causes two solutions for the cloud-base pressure in both cases at 716 cm^{-1}, a representative "far-sighted" wavenumber. We call a wavenumber far-sighted if the *e*-folding distance of transmission into the atmosphere is typically greater than the height of the surface-based inversion and "near-sighted" if only radiance from the within the inversion reaches the interferometer. Assuming the SPWO observations to be correct, the solution on 8 June is the intersection at the lower pressure (higher altitude), whereas on 7 July the higher-pressure solution (lower height) is correct (indicated by the filled circles in Fig. 4). (Figure 4b also illustrates the reason for slope-weighting of the pressure solutions at different wavenumbers. The pressure of the high-pressure solution is
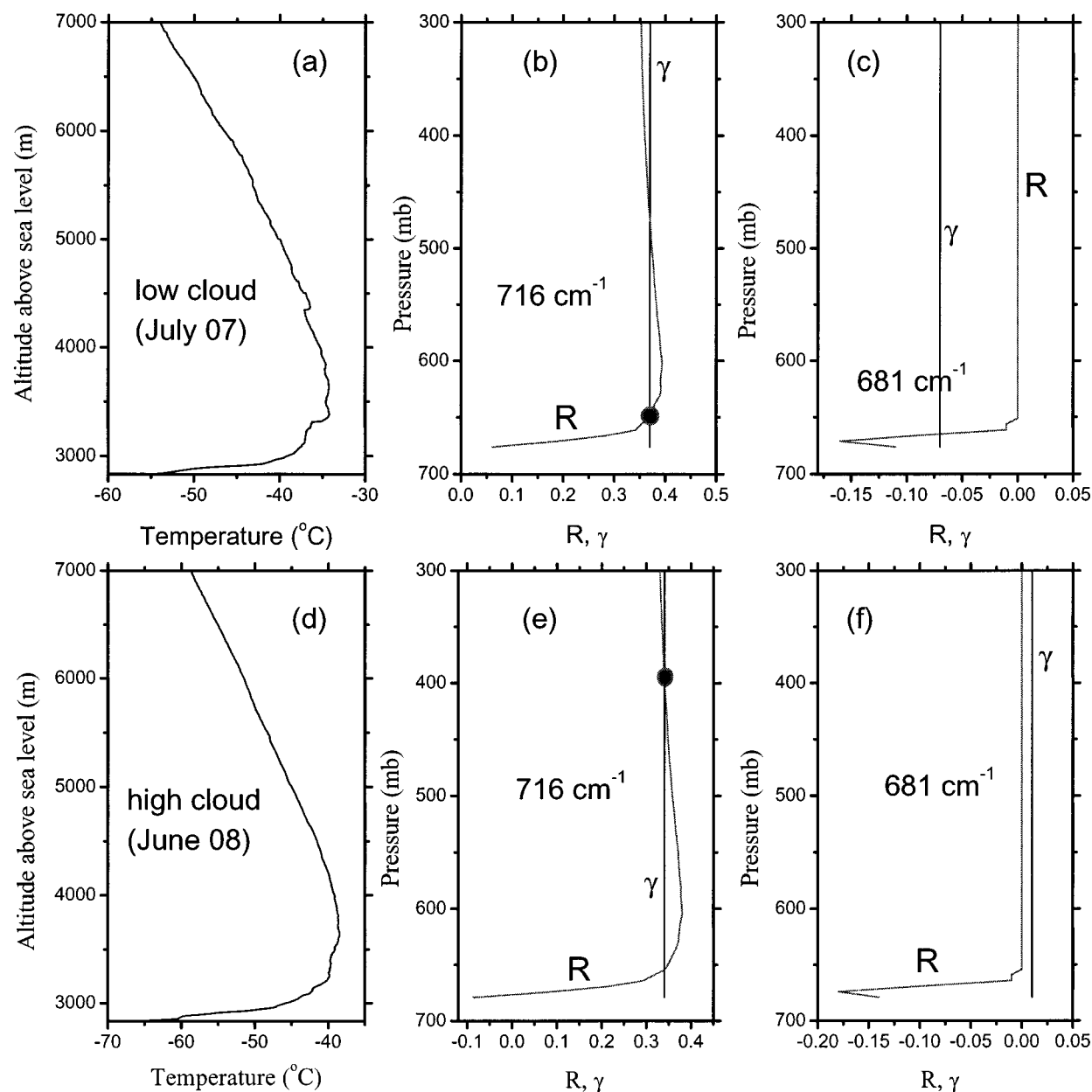
FIG. 4. Determination of cloud-base height in winter. Temperature profiles on two different days, (a) one when the cloud base is estimated to be below the inversion and (b) one when the cloud base is estimated to be above the inversion, are shown. Curves of γ and R, plotted against pressure, are shown (c), (f) at a near-sighted wavenumber (681 cm^{-1}) and (b), (e) at a far-sighted wavenumber (716 cm^{-1}). Only the Jul cloud is detectable at the near-sighted wavenumber; the Jun cloud is well beyond the e-folding distance of atmospheric transmission at this wavenumber. Both solutions are obtained at the far-sighted wavenumber. Depending on whether the cloud is detected at the near-sighted wavenumber, the appropriate solution (filled circle) is chosen at the far-sighted wavenumber.

much better defined than that of the low-pressure solution, for a small uncertainty in γ.)

To resolve the ambiguity without reference to the visual observations, we use near-sighted wavenumbers (670–700 cm^{-1}), which are sensitive only to clouds within the inversion. At these wavenumbers, almost none of the emission from above the inversion reaches the interferometer. As seen in Fig. 4 at 716 cm^{-1}, the e-folding distance of transmission into the atmosphere

includes both solutions. This is generally true for all wavenumbers between 700 and 755 cm^{-1}. At smaller wavenumbers, the increased opacity of the atmospheric CO_2 eliminates the more distant solution. The curves or R and γ at the representative near-sighted wavenumber of 681 cm^{-1} illustrate this point. In the July case, γ and R intersect, indicating a cloud within the inversion layer. In the June case, when the cloud is well above the inversion, there is no intersection of γ and

TABLE 1. Uncertainties in cloud-base pressures for individual test cases due to uncertainties in the vertical profile of temperature $T(z)$, the emissivity ratio $\varepsilon/\varepsilon_0$, the zenith angle of observations θ, the CO_2 concentration, and the measured radiance I_{obs}. The retrieved cloud-base pressure is p_c, the cloud-base height is Z_B, and H is the height of the top of the inversion. Uncertainties are shown for three zenith angles.

Test case	Z_B (m)	p_c (hPa)	H (m)	Input quantitiy	Uncertainty in cloud-base pressure (hPa)		
					45°	60°	75°
26 Jan 1992	945	603	—	$T(z)$	11	—	13
				$\varepsilon/\varepsilon_0$	10	—	9
				θ	7	—	11
				CO_2	1	—	1
				I_{obs}	8	—	9
				Total	18		21
8 Jun 1992	2112	501	650	$T(z)$	29	26	28
				$\varepsilon/\varepsilon_0$	13	14	17
				θ	15	22	27
				CO_2	3	3	5
				I_{obs}	17	12	21
				Total	39	39	47
10 Jul 1992	918	593	330	$T(z)$	22	21	29
				$\varepsilon/\varepsilon_0$	13	19	29
				θ	11	23	35
				CO_2	3	8	5
				I_{obs}	12	25	22
				Total	30	45	58
16 Jul 1992	139	663	550	$T(z)$	11	13	17
				$\varepsilon/\varepsilon_0$	5	7	7
				θ	3	9	13
				CO_2	1	1	3
				I_{obs}	6	6	5
				Total	14	18	23

R. Instead R merely approaches γ. In the absence of errors, γ and R would become equal beyond the distance of maximum transmission at near-sighted wavenumbers. When the cloud is above the inversion as in Fig. 4f, errors, which can be both positive and negative, can cause γ and R to intersect at a few wavenumbers. If, on the other hand, the cloud is below the inversion as in Fig. 4c, such intersections are much more likely, because not all negative errors in γ will eliminate the solution, and most positive errors will not destroy the intersection (unless the errors are large). Thus, the percentage of near-sighted wavenumbers at which a cloud is detected is large when the cloud base is within the inversion and small when the cloud base is above the inversion. Visual estimates of cloud-base height, made by the SPWO as well as by us, were also used in 11 of the 223 cases to resolve ambiguities.

When surface-based temperature inversions are present, distinctions between multiple solutions are possible using wavenumbers at which only one of them is detectable. From satellites, however, it would be necessary to find wavenumbers at which the e-folding distance of transmission into the atmosphere from the satellite extends to the cloud above the inversion but not to the one below it, which would be extremely difficult even with high-resolution spectral data.

c. Uncertainties

Uncertainties in cloud-base heights derived by the radiance-ratioing method are estimated using test cases.

Uncertainties in radiance measurements I_{obs}, concentrations of CO_2, and the temperature profile all cause variations in the points of intersection of R and γ. In addition, the viewing zenith angle is uncertain by $\pm 1.5°$. For observations at $\theta = 75°$, this is a significant source of uncertainty in cloud-base heights. Another important source of uncertainty is the variation in cloud emissivity between the reference wavenumber (811 cm^{-1}) and the wavenumbers used to determine cloud-base height (700–755 cm^{-1}). Although emissivities in the wings of the 15-μm band of CO_2 differ from the window emissivities by 10% or more (Wielicki and Coakley 1981), most of this difference (7%) occurs at wavenumbers greater than 811 cm^{-1} (Wu 1987). Using a reference wavenumber at 811 cm^{-1}, we estimate the average uncertainty in the ratio $\varepsilon/\varepsilon_0$ to be 3% across the wavenumber region from 700 to 755 cm^{-1}.

One source of uncertainty we do not consider is that a change in tropospheric humidity between the time of the radiosonde launch and the FTIR observation could cause a change in the clear-sky window radiance at 811 cm^{-1}. This source of uncertainty could be significant in warmer, more humid, atmospheres but is unimportant on the Antarctic Plateau, over which water-vapor emission at 811 cm^{-1} is always extremely small.

Table 1 shows the uncertainties in cloud-base pressures due to all the sources considered. In each case, these quantities were perturbed by the magnitude of the estimated uncertainties, both positive and negative, and

TABLE 2. Comparisons of cloud-base heights derived from the radiance-ratioing method with measurements from other sources.

Time	Z_B from radiance ratioing (m)	Z_B from other sources (m)	Time between two observations (h:min)	Time between radiosonde and spectral measurements (h:min)
20 Jan 1992	400	270	0:15	0:10
15 Feb 1992	90	180	0:05	0:10
3 Jun 1992	160	240	11:45	1:50
4 Jun 1992	190	390	0:25	1:45
29 Dec 1992	2270	1350*	0:15	0:20
7 Jan 1993	120	360**	1:00	0:20

* The nearest surface observation of cloud-base height was reported 20 min after the spectral data were taken. The earlier observation, made 40 min before the spectral data were taken, reports the cloud-base height at 1800 m, which agrees better with the value derived from radiance ratioing.

** Broken clouds were reported at this height. One other simultaneous cloud-base height (at 900 m) was also reported. However, this second value was reported as estimated, not measured. It is not known which of these two clouds was in our field of view.

the cloud-base pressures were recalculated. Uncertainties in CO_2 concentration cause small errors in cloud-base pressures, but uncertainties in the temperature profile and the angle of observation can result in uncertainties of up to 35 hPa. Because of errors in various input quantities, solutions may not be obtained at all wavenumbers; that is why the uncertainties in these test cases are not monotonic with angle. The bases of low clouds are more accurately derived than those of high clouds; a given change in temperature, which is the variable in the radiance-ratioing process, corresponds to a small change in pressure below the inversion, but higher in the atmosphere the same change in temperature corresponds to a larger change in pressure, because the lapse rate is not so large. Generally, the uncertainty in cloud-base pressure is found to be approximately 20–25 hPa for low clouds and 30–55 hPa for high clouds; uncertainties are also greater at larger viewing zenith angles (25–55 hPa) than at smaller angles (20–40 hPa).

Uncertainties in base height also result from the fact that clouds over the Antarctic Plateau are often thin, with optical depths τ of less than 1 (Mahesh et al. 2001). The cloud base obtained in such cases may not lie close to the actual cloud base. The solution is instead obtained as the effective temperature at which the cloud radiates and could be well above the cloud base. This means that the actual cloud base is no higher than the heights we obtain here. Radiosonde temperature profiles indicate that cloud thicknesses are typically less than 1 km, and the difference between the cloud-base heights obtained here and the level of lowest condensate is not large. Also, even in the case of thin clouds, when there is only one cloud layer in the atmosphere, the base height obtained by radiance ratioing is bounded by the range of temperatures that occur within that cloud. When there is more than one layer of cloud, however, the cloud-base height obtained will be between the base heights of the cloud layers and could be at levels where no cloud is present. However, this is unlikely because low clouds are in general optically thicker than high clouds (see Part II). Further research is necessary to determine how frequently multilayer clouds occur.

d. Verification

On six occasions during the field program, the cloud-base height was determined directly by other methods. On occasion, the SPWO launches ''pilot balloons'' with a known ascent rate, which allow the cloud-base height to be estimated by measuring the time from launch until the balloon disappears into the cloud. In addition, incoming aircraft occasionally report the cloud-base height as they descent through the cloud. Table 2 shows our estimates of cloud-base height in comparison with the values obtained from these other sources. Some of the differences may be attributed to changing cloud conditions.

Another method for verification of the radiance-ratioing method is to use a comparable dataset from a different location. Using data taken in 1996 with the Atmospheric Emitted Radiance Interferometer (AERI) at the Southern Great Plains (SGP) site of the Atmospheric Radiation Measurement (ARM) Program, we derive cloud-base heights using the radiance-ratioing method and compare those heights with lidar measurements made concurrently by a micropulse lidar (Spinhirne 1993).

Over a 2-week period during which clouds at different heights were seen, interspersed with periods of clear skies, we typically obtained cloud-base heights close to those reported by the lidar. In addition, we used several AERI measurements from a 6-h period when the cloud-base height remained steady at about 700 m above the surface and were able repeatedly to obtain the same cloud base using radiance ratioing. Comparisons were made at the times of radiosonde launches to keep uncertainties in the vertical temperature profile to a minimum. Table 3 shows a comparison of cloud-base heights obtained by radiance ratioing with those reported by the lidar. The lidar data have coarse vertical resolution (300 m), and our values all lie within this uncertainty.

The radiance-ratioing method produces solutions that are directly related to the temperature profile of the cloud base. At the ARM site, the lapse rates in the

TABLE 3. Cloud-base heights obtained by the radiance ratioing method as compared with those obtained by lidar at the ARM SGP site in Oklahoma for both selected clouds and a persistent uniform cloud deck. The resolution of the lidar reports is 300 m.

Cloud conditions	Date and time (UTC)	Z_B (lidar) (m)	Z_B (radiance ratioing) (m)
Present cloud over 6-h period	1 Nov 1996, 0531	720	710
	1 Nov 1996, 0644	1020	820
	1 Nov 1996, 0808	1020	800
	1 Nov 1996, 0928	1020	880
	1 Nov 1996, 1105	1020	800
	1 Nov 1996, 1155	1020	870
Selected clouds at different heights	28 Oct 1996, 1332	720	560
	9 Nov 1996, 0529	2820	2640
	7 Nov 1996, 1331	2820	2810

atmospheric temperature profile are smaller than at the South Pole, introducing greater uncertainty in the derived cloud-base height. When lapse rates are small, γ and R intersect at a smaller angle, and a given uncertainty in the measurement causes a large error in the derived cloud-base height. On the other hand, there is usually no surface-based inversion at the ARM site, which removes the ambiguity frequently encountered at the South Pole. Without the inversion, isothermal layers are also rare, whereas at the South Pole, the occasional broad nose of the inversion causes errors in cloud-base height determined by the radiance-ratioing method.

5. Results

Clouds were detected in the radiance spectra in 223 observations, which is about 40% of all observations made during the year. This number corresponds well to the average cloud cover reported by visual observers of 43% (Hahn et al. 1995, their Fig. 13b). Figure 5 shows the cloud-base heights determined from these observations. The seasons in Fig. 5 correspond to temperature regimes at the South Pole (Fig. 2 of Schwerdtfeger 1977; Warren 1996); a long 6-month winter of very low temperatures, 2 months of spring during which the temperature rises, 2 summer months, and 2 months of autumn during which the temperature drops again. Cloud bases are higher in spring and summer than in winter. In winter, clouds are often seen in the lowest 500 m, with bases within the surface-based temperature inversion. It is possible that seasonal differences in cloud-base heights seen in Fig. 5 are particular to 1992. Therefore, it will be useful to obtain additional years of data.

Figure 6 shows frequency distributions of the base heights obtained from all observations of clouds during the year, plotted seasonally. Cloud-base heights are distributed into two distinct modes in all seasons except summer. Clouds are often seen in the lowest 500 m, typically within the surface-based inversion. A second mode, of higher clouds, is also seen distributed over a much wider range of base heights in the nonsummer months. During the summer months, cloud-base heights are distributed over a range of heights that spans both modes seen during the other times of the year. The lowest cloud is almost always within 5 km of the surface (8 km above sea level). The tropopause at the South Pole is typically 5–6 km above the surface (Warren 1996, his Fig. 3), so all the clouds whose bases were located by the radiance-ratioing method are in the troposphere. "High" clouds on the Antarctic Plateau are thus lower than elsewhere on the earth, where the high
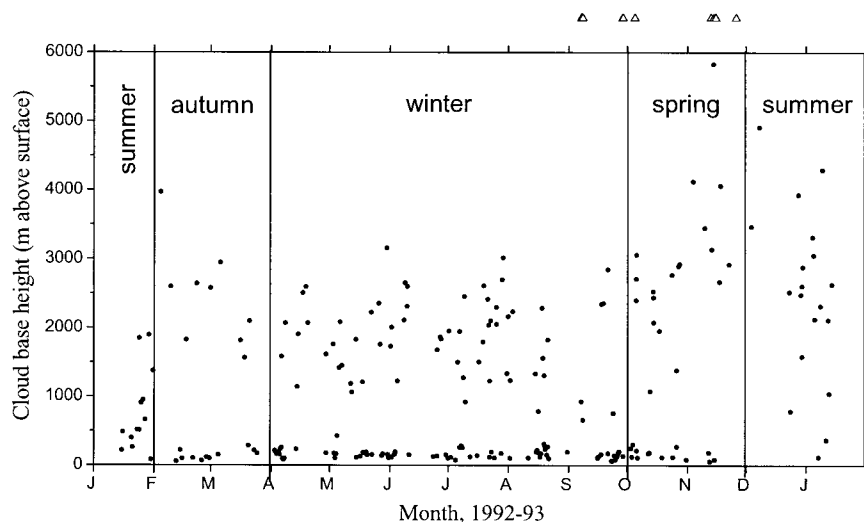

FIG. 5. All retrieved cloud-base heights during the year. Tick marks on the horizontal axis mark the beginning of each month. Cloud bases are higher in summer than in winter. The clouds were especially high during times when there was no surface-based inversion (Dec 1992). PSCs can be detected by radiance ratioing, but the method is not appropriate to locate their bases reliably. Observations of PSCs are shown as open triangles above the figure.
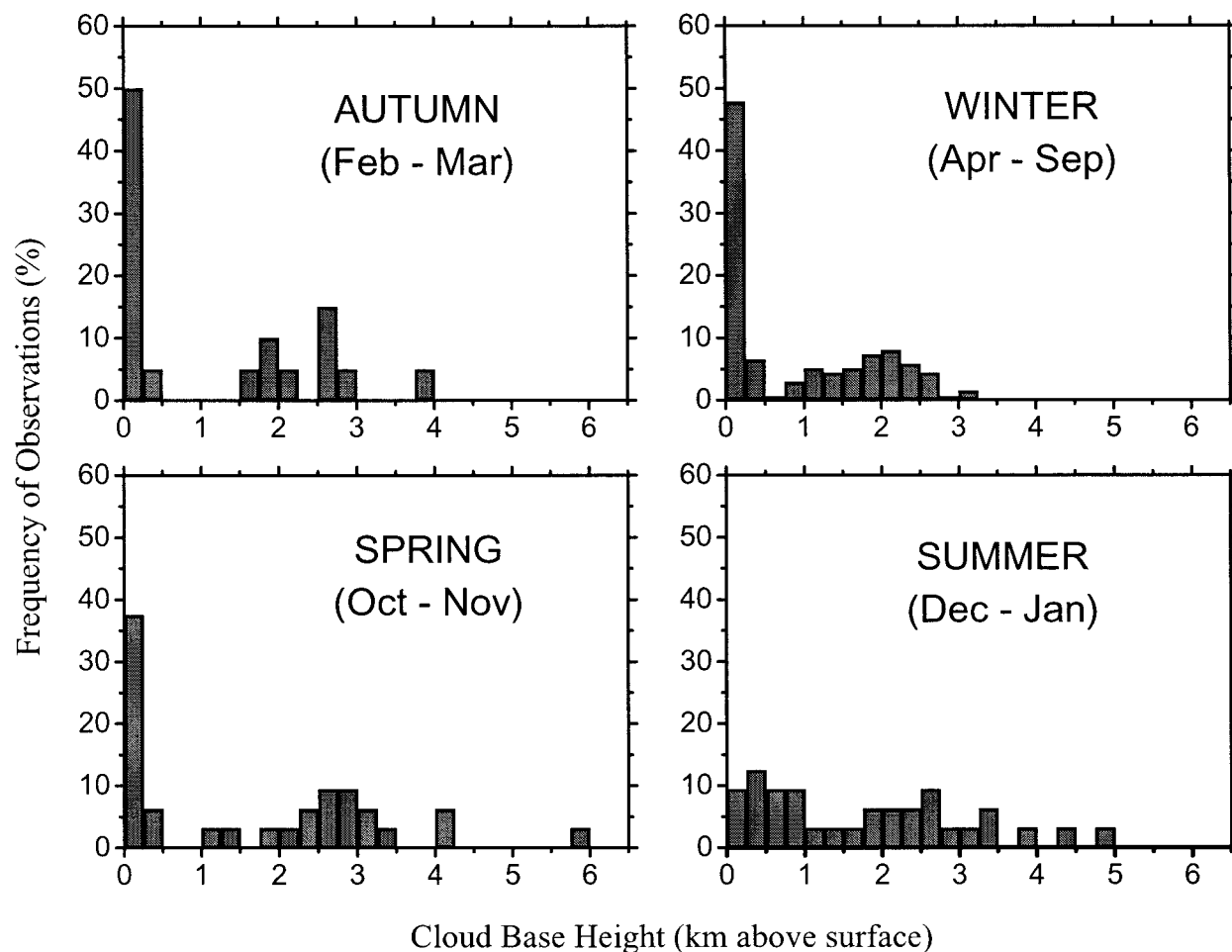
FIG. 6. Histograms of cloud-base heights at the South Pole during 1992, for each of four seasons.

cloud level usually refers to clouds with bases more than 6 km above surface (World Meteorological Organization 1956, p. 8), The bimodality of the distribution is discussed later.

At wavenumbers larger than 755 cm^{-1}, the e-folding distance of transmission into the atmosphere is several tens of kilometers or more, and at these wavenumbers polar stratospheric clouds (PSCs) can be detected. However, their emission is so weak that the radiance-ratioing method cannot be used to determine their base heights. Observations of PSCs are shown outside the range of the vertical axis in Fig. 5, indicating that the base heights exceed 6 km but cannot be quantified. Intersections of R and γ correspond to specific temperatures in the atmosphere; because PSCs are typically much colder than any tropospheric clouds, they can be detected by this method. To locate their base heights accurately, however, we would require sufficient wavenumbers at which atmospheric transmission extends beyond the troposphere, but not much farther than the height of a typical PSC. There are only a few wavenumbers at which the e-folding distance of transmission into the atmosphere

is comparable to the typical base heights of PSCs. The weighting functions, even at these few wavenumbers, are fairly broad. Broad weighting functions introduce too much uncertainty to be useful in detecting cloud-base heights accurately in the stratosphere.

The cloud-base heights presented so far do not constitute even a 1-yr weather description because data from some days are missing. The interferometer had to be turned off during blizzards because its external mirror became coated with blowing snow, and it was also shut down for a few other brief periods. To obtain more representative results, periods of missing data are filled. Each day, the instrument was scheduled to make two observations, beginning at 1000 UTC and 2200 UTC. A total of 732 cases would therefore be necessary to compile a descriptive dataset for the entire year. Our FTIR dataset comprises 516 observations; missing values are filled as follows. In blizzard conditions, the instrument was turned off, and then it was restarted immediately following each blizzard. We assumed that, throughout the blizzard, cloud conditions were unchanged from the last observation immediately prior to

TABLE 4. Monthly average cloud-base heights (Z_B, in meters above the surface) obtained at the South Pole. On days when spectral observations were not available, persistence was used to assign base heights. (01/92 is Jan 1992, etc.)

Month	Z_B (m)
01/92	800
02/92	1300
03/92	1200
04/92	1000
05/92	700
06/92	600
07/92	1200
08/92	400
09/92	800
10/92	1100
11/92	2600
12/92	2000
01/93	2200

the blizzard. Other missing values were filled in a similar manner, but there were very few missing data on non-blizzard days, so the results are not sensitive to this procedure. An annual cycle of cloud-base heights, developed using such "persistence" criteria, is shown in Table 4.

6. Discussion

The bimodal distribution of cloud-base heights, shown in Fig. 6, has important implications for modeling of Antarctic climate and is contrary to earlier results. Stone (1993), using a small set of data, reported that the cloud base is typically at the top of the inversion. The bimodal distribution we find, in contrast, suggests that whereas base heights are either above or below the inversion, they are rarely at the top of the inversion. Therefore, we now examine the sensitivity of the bimodal distribution of the cloud-base heights and show that it is not an artifact of the radiance-ratioing method.

Using calculations of cloud radiance from modeled clouds and perturbations of the atmospheric temperature profile, we examined the errors in cloud-base height that would be caused by perturbations of 3 K in the lowest 1 km of the atmosphere. The average uncertainty in cloud-base height, for a cloud whose true base height is exactly at the top of the inversion, is at most 20 hPa, or about 150–200 m. Because of measurement errors, a cloud whose base is exactly at the top of the inversion will usually give two solutions of base height where γ is equal to R, one above and the other below the top of the inversion. Lapse rates below the top of the inversion are very steep, and a temperature error of 3 K is unlikely to affect the determination of cloud-base height by more than 5–10 hPa. A cloud exactly at the top of the inversion is likely to be detected by several near-sighted wavenumbers. As a result, the radiance-ratioing method would determine the cloud-base height as the solution below the top of the inversion rather than the one above the inversion. Steep lapse rates within the inversion limit

the error in cloud-base height when the solution below the inversion is chosen.

On the other hand, if we were to choose the solution above the inversion, uncertainties as large as 25 hPa are possible with a temperature uncertainty of 3 K because lapse rates above the inversion are much less steep. However, in most of the cases, the radiance measurements were made coincident with the radiosonde launch, and the temperature errors we permitted in these simulations (± 3 K) are extremely generous. We thus conclude that temperature errors will not cause the shape of the distribution in Fig. 6 to change much. This conclusion can also be verified by examining how the distribution of base heights might look if, the fact, cloud bases are exactly at the top of the inversion instead of where we diagnose them to be.

The three parts of Fig. 7 illustrate this approach. In Fig. 7a, the distribution of base heights diagnosed by our method is shown; this is just the sum of all four panels of Fig. 6. We then considered the subset of cases for which the cloud base is more than 200 m from the top of the inversion but the difference between the temperature at cloud base and the temperature at the top of the inversion is less than 3 K. These cases represent the subset of our observations that are most likely to be affected by the fact that our method does not determine base heights that are exactly at the top of the inversion and instead moves them away. A height difference of less than 200 m is not significant, because errors due to input parameters can cause comparable uncertainty in our determination of cloud-base height, and similar uncertainties due to the method itself do not worsen the determination of cloud-base height any further.

Assuming that this subset of cloud-base heights has been erroneously determined, we reset the base heights for each of these clouds to the top of the inversion on that day. The resulting distribution of base heights (Fig. 7b) is not greatly altered, and still retains a bimodal appearance. Even if we grossly exaggerate this experiment and reset all values of cloud base within 6 K of the inversion temperature to the top of the inversion, the bimodal nature is still retained (Fig. 7c). These experiments exaggerate the impact of errors due to the method by being generous in choosing the subset. Yet the bimodal distribution persists, indicating that the distribution of base heights shown in Fig. 6 is not an artifact of our method.

In addition, it is important to keep in mind that the bimodal distribution is a distribution of base heights, and it is probable that in the cases where the base height is below the inversion the cloud itself extends through the top of the inversion. The average height of the inversion is about 600–650 m, and even thin clouds with bases below the inversion can reasonably be assumed to extend beyond the top of the inversion.

The visual estimates of cloud-base height made by the observers at the SPWO also show a bimodal distribution. However, the absolute values of such obser-
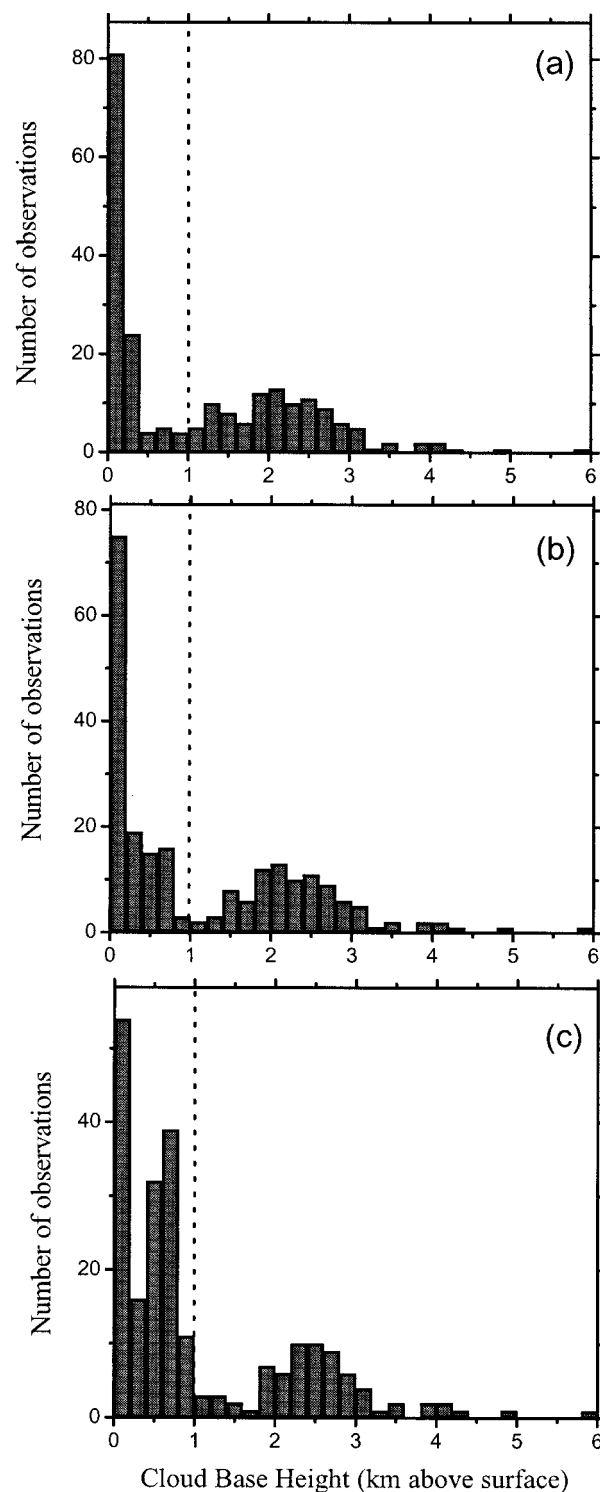
FIG. 7. Tests to determine whether the bimodal distribution of cloud-base heights obtained by radiance ratioing is an artifact. (a) The sum of all four panels of Fig. 6, showing the distribution of cloud-base heights obtained from the spectral measurements. (b) Cloud-base heights more than 200 m above or below the top of the inversion but at temperatures within 3 K of the temperature at the top of the inversion have been reset to the height of the inversion on that day, creating more entries in the bins of typical inversion height
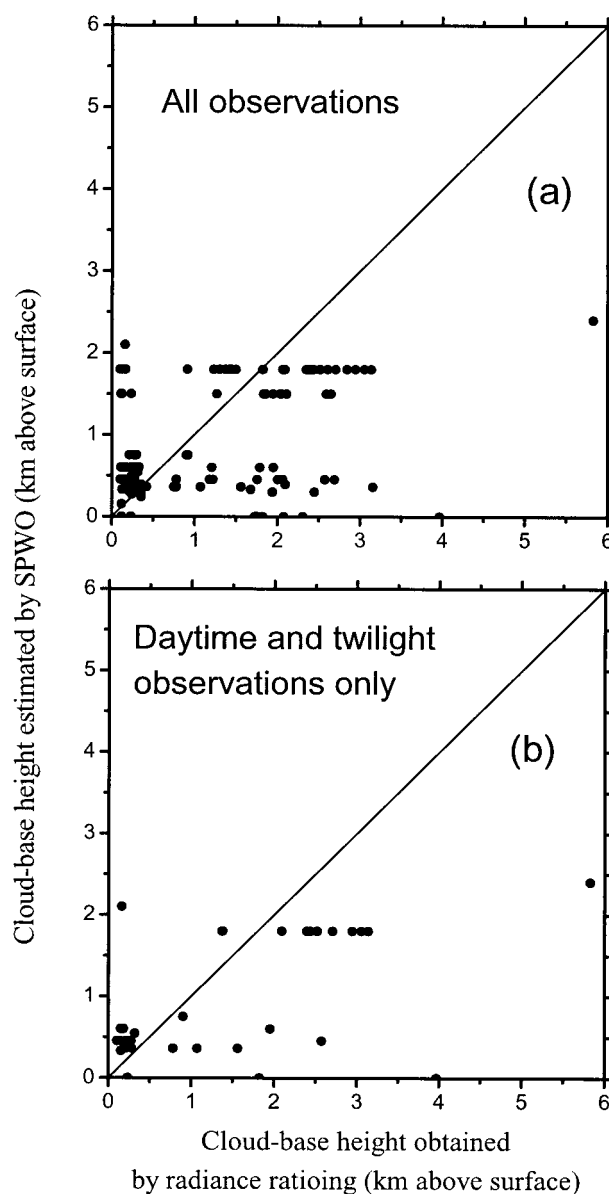
FIG. 8. Estimates of cloud-base heights made by the observers at the SPWO as compared with base heights derived by radiance ratioing. Comparisons were made only for those cases when the SPWO report was made within 2 h of the FTIR measurement. In many cases, the SPWO report is within 0.5 h of the radiance measurement. The weather observers tend to underestimate the base heights of the high clouds and overestimate the heights of the low clouds relative to the base height inferred from radiance ratioing.

←

(400–800 m). (c) The condition for resetting the cloud-base heights to the inversion heights is further relaxed to include clouds whose base temperature is within 6 K of the inversion-top temperature. The bimodal distribution still persists, indicating that it is not an artifact of the radiance-ratioing method. The vertical dashed line indicates the average height of the inversion top.

vations are not very reliable. Figure 8a shows the estimates of cloud-base heights made by observers at the SPWO, along with our values derived from radiance ratioing. Comparisons were made only for the cases for which the SPWO observations were within 2 h of the FTIR measurement. The observers at the SPWO estimate the base height in hundreds of feet above the surface. The strings of values at 1500 m and 1800 m are reports of 5000 feet and 6000 feet. The average cloud-base height from visual observations is close to that from radiance ratioing, but the individual values are uncorrelated. In the absence of reference objects, such as mountains or tall structures, the observers have no reliable way of making estimates of cloud-base heights, and this situation is clearly seen in the figure. Figure 8b limits the comparison to the observations made under conditions of good illumination of the clouds, which should facilitate their identification by visual observation. There is still no correlation of the SPWO base heights with the FTIR base heights, but the bimodal distribution persists.

7. Conclusions

Cloud-base heights can be determined from surface spectral measurements of longwave emission by radiance ratioing, a technique originally developed for the determination of cloud-top heights from satellite data. To resolve ambiguity in the retrieval, a variation on the radiance-ratioing method has been developed here that permits clouds above the surface-based inversion to be distinguished from those below it. In all seasons except summer, clouds apparently form in two distinct modes, one with base heights below the surface-based inversion and the other with bases 2–3 km above the surface. We do not have an explanation for why these two modes exist, but this result is consistent with visual observations. Research into cloud formation mechanisms over the plateau is needed to explain the distribution of base heights.

REFERENCES

Chahine, M. T., 1974: Remote sounding of cloudy atmospheres. I. The single cloud layer. *J. Atmos. Sci.,* **31,** 233–243.

Clough, S. A., M. J. Iacono, and J. L. Moncet, 1992: Line-by-line calculations of atmospheric fluxes and cooling rates: Application to water vapor. *J. Geophys. Res.,* **97,** 15 761–15 785.

Frey, R., 1988: On the determination of cloud altitude using infrared spectral radiances. M.S. thesis, Dept. of Atmospheric and Oceanic Sciences, University of Wisconsin—Madison, 52 pp.

Hahn, C. J., S. G. Warren, and J. London, 1995: The effect of moonlight on observation of cloud cover at night, and application to cloud climatology. *J. Climate,* **8,** 1429–1446.

King, M. D., Y. J. Kaufman, W. P. Menzel, and D. Tanre, 1992: Remote sensing of cloud, aerosol, and water vapor properties from the Moderate Resolution Imaging Spectrometer (MODIS). *IEEE Trans. Geosci. Remote Sens.,* **30,** 2–27.

Lubin, D., 1994: Infrared properties of the maritime Antarctic atmosphere. *J. Climate,* **7,** 121–140.

——, and D. A. Harper, 1996: Cloud radiative properties over the South Pole from AVHRR infrared data. *J. Climate,* **9,** 3405–3418.

——, B. Chen, D. H. Bromwich, R. C. J. Somerville, W. Lee, and K. M. Hines, 1998: The impact of Antarctic cloud radiative properties on a GCM climate simulation. *J. Climate,* **11,** 447–462.

Mahesh, A., V. P. Walden, and S. G. Warren, 1997: Radiosonde temperature measurements in strong inversions: Correction for thermal lag based on an experiment at the South Pole. *J. Atmos. Oceanic Technol.,* **14,** 45–53.

——, ——, and ——, 2001: Ground-based infrared remote sensing of cloud properties over the Antarctic Plateau. Part II: Cloud optical depths and particle sizes. *J. Appl. Meteor.,* **40,** 1279–1294.

McCleese, D. J., and L. S. Wilson, 1976: Cloud top heights from temperature sounding instruments. *Quart. J. Roy. Meteor. Soc.,* **102,** 781–790.

Menzel, W. P., W. L. Smith, and T. R. Stewart, 1983: Improved cloud motion wind vector and altitude assignment using VAS. *J. Appl. Meteor.,* **22,** 377–384.

Schwerdtfeger, W., 1977: Temperature regime of the South Pole: Results of 20 years' observations at Amundsen–Scott Station. *Antarct. J. U. S.,* **12,** 156–159.

Simmonds, I., 1990: Improvements in general circulation model performance in simulating Antarctic climate. *Antarct. Sci.,* **2,** 287–300.

Smith, W. L., and C. M. R. Platt, 1978: Comparison of satellite-deduced cloud heights with indications from radiosonde and ground-based laser measurements. *J. Appl. Meteor.,* **17,** 1796–1802.

——, and R. Frey, 1990: On cloud altitude determinations from high-resolution interferometer sounder (HIS) observations. *J. Appl. Meteor.,* **29,** 658–662.

——, H. M. Woolf, P. G. Abel, C. M. Hayden, M. Chalfant, and N. Grody, 1974: *Nimbus-5* sounder data processing system. Part I: Measurement characteristics and data reduction processes NOAA Tech. Memo. NESS 57, 99 pp.

Spinhirne, J. D. 1993: Micropulse lidar. *IEEE Trans. Geosci. Remote Sens.,* **31,** 48–55.

Stone, R. S., 1993: Properties of austral winter clouds derived from radiometric profiles at the South Pole. *J. Geophys. Res.,* **98,** 12 961–12 971.

Walden, V. P., 1995: The downward longwave radiation spectrum over the Antarctic Plateau. Ph.D. thesis, Geophysics Program, University of Washington, 267 pp.

——, S. G. Warren, F. J. Murcray, and R. G. Ellingson, 1997: Infrared radiance spectra for testing radiative transfer models in cold and dry atmospheres: Test cases from the Antarctic Plateau. *Bull. Amer. Meteor. Soc.,* **78,** 2246–2247.

——, ——, and ——, 1998: Measurements of the downward long-

wave radiation spectrum over the Antarctic Plateau and comparisons with a line-by-line radiative transfer model for clear skies. *J. Geophys. Res.,* **103,** 3825–3846.

Warren, S. G., 1996: Antarctica. *Encyclopedia of Climate and Weather,* S. H. Schneider, Ed., Oxford University Press, 32–39.

Wielicki, B. A., and J. A. Coakley Jr., 1981: Cloud retrieval using infrared sounder data: Error analysis. *J. Appl. Meteor.,* **20,** 157–169.

World Meteorological Organization, 1956: *The International Cloud Atlas.* Vol. I, World Meteorological Organization, 155 pp.

Wu, M.-L. C., 1987: A method for remote sensing the emissivity, fractional cloud cover and cloud top temperature of high-level, thin clouds. *J. Climate Appl. Meteor.,* **26,** 225–233.

Yamanouchi, T., K. Suzuki, and S. Kawaguchi, 1987: Detection of clouds in Antarctica from infrared multispectral data of AVHRR. *J. Meteor. Soc. Japan,* **65,** 949–962.